

[[Fe(CO)₃]₄{SnI₆I₄}²⁻: The First Bimetallic Adamantane-Like Cluster

Silke Wolf,^[a] Florian Winter,^[b] Rainer Pöttgen,^[b] Nils Middendorf,^[c] Wim Klopper,^[c] and Claus Feldmann*^[a]

Adamantane (i.e., tricyclo[3.3.1.1^{3,7}]decane) represents the base body of tetracyclic alkanes and the smallest species of a diamondoid compound. This very stable, high-symmetry constitution is characteristic for well-known molecular compounds, ranging from urotropine N₄(CH₂)₆ or the phosphor oxides P₄O₆/P₄O₁₀ even to several pharmaceutical agents.^[1] Closely related to carbon, the outstanding sila-adamantane {Si(SiMe₃)₄SiMe₂}₆ has been discovered recently.^[2] Adamantane-like cages are, moreover, widely found for compositions M₄X₆ (M: metal, X: N, P, O, S, Se, Te).^[3] In view of this commonness, it is surprising that neither any adamantane-like cluster composed of real metals nor any bimetallic cluster has been identified to date. This is even more interesting since the high symmetry and the approximated spherical shape of the adamantane cage are often accompanied by a comparably low reactivity and a certain stability.

Here, we report on [BMIm]₂[[Fe(CO)₃]₄Sn₆I₁₀] (**1**) and [BMIm]₆[S][{Fe(CO)₃]₄Sn₆I₁₀]₂ (**2**) (BMIm: 1-butyl-3-methylimidazolium) containing [[Fe(CO)₃]₄{SnI₆I₄}²⁻ as the first adamantane-like (metal) cluster (Figure 1). Both compounds were obtained by treating Fe(CO)₅ and SnI₄ in the ionic liquids [BMIm][NTf₂] and [BMIm][OTf] (NTf₂: bistrifluoromethanesulfonimide; OTf: triflate). Structure, bonding and valence state of the [[Fe(CO)₃]₄{SnI₆I₄}²⁻ cluster were validated based on structure analysis, infrared and ¹¹⁹Sn Mössbauer spectroscopy, as well as by density functional theory (DFT).

In principle, Fe–Sn carbonyl clusters are well-known and have been widely studied; their structural, magnetic, catalytic and optical properties have been examined intensely. Most often, four-membered Fe₂Sn₂ rings as well as bent

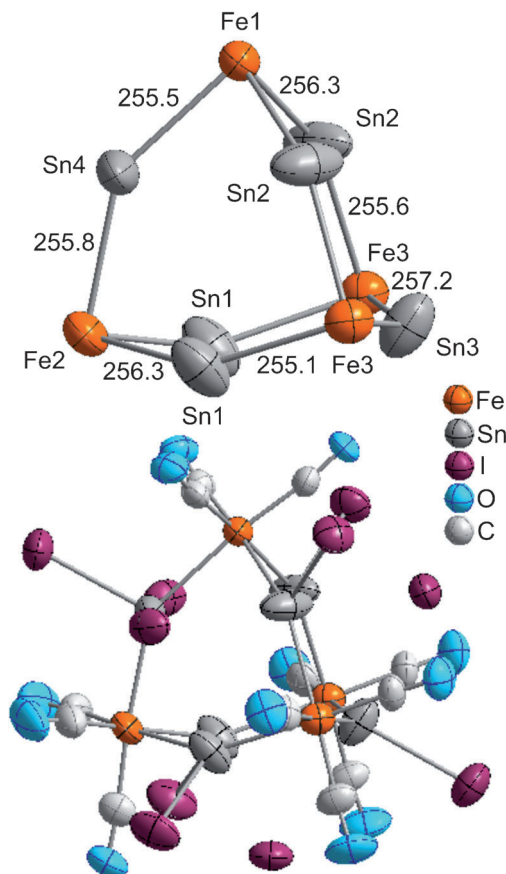


Figure 1. Molecular structure of the [[Fe(CO)₃]₄{SnI₆I₄}²⁻ cluster in **1** (selected distances in pm, deviation ±0.1 pm; see the Supporting Information for details).

Sn–Fe–Sn or Fe–Sn–Fe strings have been described.^[4] Larger Fe–Sn carbonyls comprise trigonal bipyramidal Fe₃Sn₂ ([{(Cp)Fe(CO)₂]₂Sn₂Fe₃(CO)₉]),^[5] tetrahedral SnFe₄ (Sn₂Fe₆(CO)₂₃),^[6] and a {Fe(CO)₂Cp}-stabilized propellane-like Sn₅ unit ([Sn₅(dep)₆]{Fe(CO)₂(Cp)₂}).^[7] A Fe₄Sn₆ cluster, as observed in **1** and **2**, is here described for the first time. Interestingly, the [[Fe(CO)₃]₄{SnI₆I₄}²⁻ cluster does not contain alkyl or aryl groups as they are typically needed for steric and/or electronical stabilization, especially, of larger Fe–Sn cluster species.

By ionic-liquid-based synthesis, [BMIm]₂[[Fe(CO)₃]₄Sn₆I₁₀] (**1**) and [BMIm]₆[S][{Fe(CO)₃]₄Sn₆I₁₀]₂ (**2**) were obtained as dark-red crystals. Both compounds are highly sensitive to moisture and oxygen. Moreover, even slight squeezing of

[a] Dr. S. Wolf, Prof. Dr. C. Feldmann
Institut für Anorganische Chemie
Karlsruhe Institute of Technology (KIT)
Engesserstraße 15, 76131 Karlsruhe (Germany)
Fax: (+49) 721-6084892
E-mail: claus.feldmann@kit.edu

[b] Dipl.-Chem. F. Winter, Prof. Dr. R. Pöttgen
Institut für Anorganische und Analytische Chemie
University of Münster, Corrensstrasse 30, 48149 Münster (Germany)

[c] Dipl.-Chem. N. Middendorf, Prof. Dr. W. Klopper
Institut für Physikalische Chemie
Karlsruhe Institute of Technology (KIT)
Fritz-Haber-Weg 2, 76131 Karlsruhe (Germany)

Supporting information for this article is available on the WWW under <http://dx.doi.org/10.1002/chem.201202683>.

the crystals led to decomposition under gas release (i.e., CO). X-ray structure analysis based on single crystals revealed the title compounds to crystallize with the space groups $P2_1/m$ (**1**) and $R\bar{3}$ (**2**; see the Supporting Information).^[8] Both contain the adamantane-like carbonyl cluster $[\{\text{Fe}(\text{CO})_3\}_4\{\text{SnI}_6\text{I}_4\}]^{2-}$ as well as $[\text{BMIm}]^+$ counterions (Figure 1). Moreover, S^{2-} anions are incorporated in **2**. The composition of both title compounds was further confirmed by energy-dispersive X-ray (EDX) analysis. The measured Fe/Sn/I ratios of 3.8:6.6:10 (**1**) and 3.6:6.7:10 (**2**; scaled on iodine as the heaviest element) fit with the calculated data (4:6:10) within the significance of measurement. EDX also indicates the presence of sulfur in **2**, which was quantified by elemental chemical analyses. Again, the experimental values ($w(\text{C})$: 14.3 %, $w(\text{H})$: 1.3 %, $w(\text{N})$: 2.8 %, $w(\text{S})$: 0.5 %) correspond well with the calculated data ($w(\text{C})$: 14.5 %, $w(\text{H})$: 1.5 %, $w(\text{N})$: 2.8 %, $w(\text{S})$: 0.5 %).

The $[\{\text{Fe}(\text{CO})_3\}_4\{\text{SnI}_6\text{I}_4\}]^{2-}$ anion constitutes an adamantane-shaped Fe_4Sn_6 cluster (Figure 1). Herein, iron is coordinated by three tin atoms and three CO ligands. All tin atoms are coordinated by two iron and one iodine atom. Hence, a distorted octahedral coordination around Fe and a distorted trigonal coordination around Sn are observed. Consequently, the Sn–Fe–Sn angles ($85.5(1)$ – $89.7(1)^\circ$) are smaller, and the Fe–Sn–Fe angles ($142.8(1)$ – $144.3(1)^\circ$) are larger as compared to the tetrahedral arrangement of all carbon atoms in adamantane. The sum of the smaller Sn–Fe–Sn and the larger Fe–Sn–Fe angles is, however, closely related to the doubled tetrahedral angle, and is thus in agreement with the overall adamantane-like shape. Finally, each of the four faces of the Fe_4Sn_6 cluster cage is capped by an additional iodine atom.

The Fe–Sn distances in the $[\{\text{Fe}(\text{CO})_3\}_4\{\text{SnI}_6\text{I}_4\}]^{2-}$ cluster in **1** and **2** range from 254.4(1) to 257.2(1) pm (Figure 1, see the Supporting Information) and match well with literature data of known Fe–Sn clusters (247–273 pm).^[4–7,9] The Fe–Sn distances of the adamantane-like Fe_4Sn_6 substructure are, furthermore, in a typical range of iron stannides, such as Fe_3Sn_2 (268–280 pm), FeSn (265–270 pm), or FeSn_2 (279 pm).^[10] The Sn–I distances of the terminal iodine atoms are found to be 273.5(1) to 275.3(1) pm. These distances are longer than in SnI_4 (263 pm), but shorter than in SnI_2 (300 pm).^[11] The iodine atoms that cap the cluster cage exhibit significantly longer Sn–I distances. Since these additional iodine atoms are slightly shifted from the center of the cluster-cage face, a group of shorter (315.2(1)–325.8(1) pm) and longer distances (340.1(1)–348.3(1) pm) occur (see the Supporting Information). Altogether, these distances correspond to the sum of the ionic radii Sn^{2+} and I^- (330 pm),^[12] and point to a predominately ionic bonding. Hence, the carbonyl cluster in **1** and **2** can be also rationalized as $[\{\text{Fe}(\text{CO})_3\}_4\{\text{SnI}_6\text{I}_4\}]^{2+}$ when considering strong covalent bonding only.

For the CO ligands in $[\{\text{Fe}(\text{CO})_3\}_4\{\text{SnI}_6\text{I}_4\}]^{2-}$, C–O distances of 111(1)–118(1) pm are observed and fit with terminally bound CO (Table 1). The mean C–O distances of 113 pm (**1**) and 116 pm (**2**) are very comparable to $\text{Fe}(\text{CO})_5$

Table 1. Comparison of experimental IR vibrations and bond lengths for **1** and **2**.

Compound	C–O bond length [pm]	Position of CO vibration [cm^{-1}]
1	110.7(1) (Fe1)	2033
	112.5(1) (Fe1)	1998
	114.8(2) (Fe2)	1984
	115.2(1) (Fe2)	
	112.1(1) (Fe3)	
	113.1(1) (Fe3)	
	113.9(1) (Fe4)	
	115.2(1) (Fe1)	2032
2	115.3(1) (Fe1)	1998
	116.6(1) (Fe1)	1986
	117.8(1) (Fe2)	
Free CO	112.8	2143
$\text{Fe}(\text{CO})_5$	114.5	2022
		2000

(115 pm; see the Supporting Information).^[13] This holds for the Fe–C distances (175(1)–181(1) pm) as well ($\text{Fe}(\text{CO})_5$ with 179 pm).^[13] According to FT-IR spectroscopy, three different CO vibrations can be resolved for **1** and **2** (Table 1, Figure 2). Corresponding to the C–O distances, the CO vibrations are in a similar wavenumber range as observed for $\text{Fe}(\text{CO})_5$. Thus, bonding situation and valence state of iron

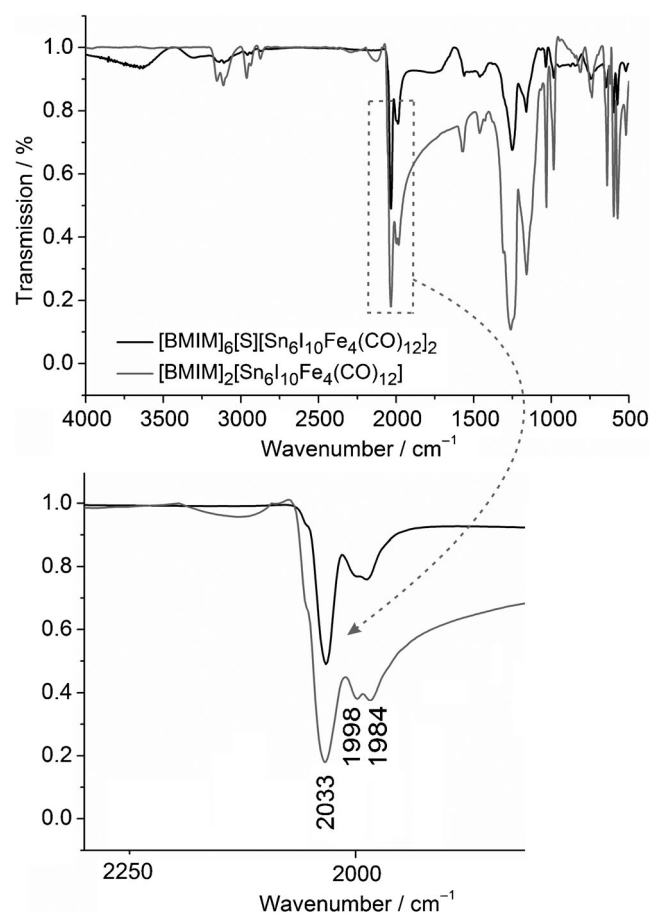


Figure 2. FT-IR spectra of $[\text{BMIm}]_2[\{\text{Fe}(\text{CO})_3\}_4\text{Sn}_6\text{I}_{10}]$ (**1**) and $[\text{BMIm}]_6[\text{S}][\{\text{Fe}(\text{CO})_3\}_4\text{Sn}_6\text{I}_{10}]_2$ (**2**).

in $[\{\text{Fe}(\text{CO})_3\}_4\{\text{SnI}_6\text{I}_4\}]^{2-}$ can be assumed to be similar to $\text{Fe}(\text{CO})_5$.

Altogether, bond lengths and angles in **1** and **2** are very similar (see the Supporting Information); this indicates that the adamantane-like $[\{\text{Fe}(\text{CO})_3\}_4\{\text{SnI}_6\text{I}_4\}]^{2-}$ cluster, as expected, is less influenced by the cation or the crystal structure. For both compounds, the large cluster cage is arranged like a dense packing of hard spheres with layer sequences AA (**1**) and ABC (**2**) as well as with $[\text{BMIm}]^+$ and $[\text{S}]^{2-}$ filling the holes (**2**) between the cluster cages (see the Supporting Information). For **1**, extensive stacking faults are found that can be related to a quasi-rectangular superstructure with $a' = 4a + c$ and $\beta' = 90.04^\circ$ (see the Supporting Information).

Based on the above bond-length considerations and the results of FT-IR spectroscopy, the valence state of iron can be concluded to be similar to $\text{Fe}(\text{CO})_5$. Thus, a formal oxidation state of $\text{Fe}^{\pm 0}$ is adopted. In view of the overall charge of the $[\{\text{Fe}(\text{CO})_3\}_4\{\text{SnI}_6\text{I}_4\}]^{2-}$ cluster, the formal oxidation state of tin then must be $\text{Sn}^{+1.3}$. To further elucidate the bonding characteristics and the formal oxidation state, density functional theory (DFT) and ^{119}Sn Mössbauer spectroscopy studies were conducted.

At the PBE0/dhf-SVP level, geometry optimization of a $[\{\text{Fe}(\text{CO})_3\}_4\{\text{SnI}_6\text{I}_4\}]^{2+}$ cluster (thus, with the capping I^- atoms subtracted) yielded a regular tetrahedron (T_d), with Fe–Sn, Sn–I, Fe–C, and C–O distances of 255.3, 268.5, 179.2, and 113.5 pm, respectively (Table 2). Hund's localization rule is

Table 2. DFT calculated Fe–C and C–O bond lengths of $[\{\text{Fe}(\text{CO})_3\}_4\{\text{SnI}_6\text{I}_4\}]^{2+}$ in comparison with selected reference compounds.

Compound	Fe–C bond length [pm]	C–O bond length [pm]	Harmonic vibrational wavenumber of CO [cm^{-1}]
CO		112.8	2274
$[\{\text{Fe}(\text{CO})_3\}_4\{\text{SnI}_6\text{I}_4\}]^{2-}$	176.8–177.0	114.4	2131–2182
$[\{\text{Fe}(\text{CO})_3\}_4\{\text{SnI}_6\text{I}_4\}]^{2+}$	179.2	113.5	2201–2240
$[\text{FeI}(\text{CO})_3(\text{SnI}_3)_2]^-$	176.3–181.2	113.8–114.1	2166–2200
$\text{Fe}(\text{CO})_5$	179.0–179.9	114.0–114.3	2145–2247
$\text{FeI}_2(\text{CO})_3$		113.2–113.7	2197–2253

obeyed, and bonding can be described fully in terms of localized 2-centre-2-electron bonds (2c2e). If we add, formally, one electron to Fe ($3d^64s^2$), it has nine valence electrons and can form nine bonds (three to Sn and $3 \times 2 = 6$ to CO with σ -donor and π -back bonding). Hence, the 18-electron rule is obeyed for Fe. Concerning Sn, we formally subtract one electron to give Sn^+ , in agreement with the total charge of the cluster, and the three valence electrons of Sn^+ form three bonds (two to Fe and one to I).

Alternatively, the Fe–Sn–Fe bridges can be described in terms of 3-centre-2-electron (3c2e) bonds. Figure 3 shows localized molecular orbitals (MOs) as obtained from a Pipek–Mezey localization procedure.^[14] On the left-hand side, Figure 3 shows two (out of six equivalent) 3c2e bonds formed with the Sn 5s orbital, and on the right, it shows the

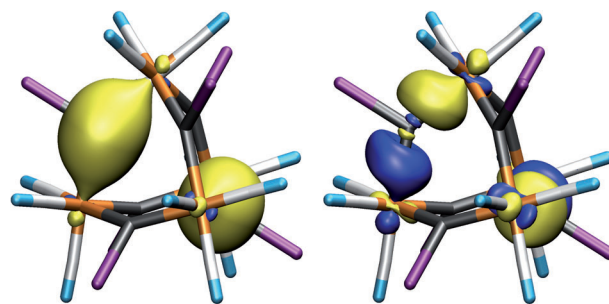


Figure 3. Pipek–Mezey localized 3c2e MOs of $[\{\text{Fe}(\text{CO})_3\}_4\{\text{SnI}_6\text{I}_4\}]^{2+}$.

corresponding bonds that involve the Sn 5p orbital. A subsequent Boys localization procedure^[15] yielded twelve equivalent 2c2e bonds. Figure 4 shows three of these twelve localized MOs.

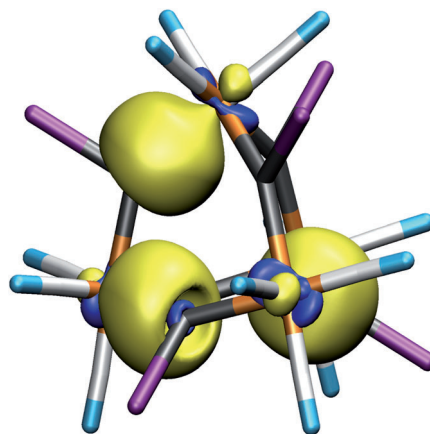


Figure 4. Boys localized 2c2e MOs of $[\{\text{Fe}(\text{CO})_3\}_4\{\text{SnI}_6\text{I}_4\}]^{2+}$.

The geometry of the dianion $[\{\text{Fe}(\text{CO})_3\}_4\{\text{SnI}_6\text{I}_4\}]^{2-}$, now including the more ionic iodine atoms that cap the cluster faces, could also be optimized. Although there is only a minor effect on the bond lengths (Table 2), the cluster symmetry is now optimized to S_4 instead of T_d . At the PBE0/dhf-SVP level, the energy difference between $[\{\text{Fe}(\text{CO})_3\}_4\{\text{SnI}_6\text{I}_4\}]^{2-}$ (T_d) and $[\{\text{Fe}(\text{CO})_3\}_4\{\text{SnI}_6\text{I}_4\}]^{2-}$ (S_4) is only 10 kJ mol^{-1} . Accordingly, the structural change from T_d to S_4 is small. It is most noticeable by a small shift of the tin atoms (see the Supporting Information). For the solid state, clusters of local S_4 symmetry most likely average in the crystal lattice to an apparent T_d symmetry. This view is validated by thermal ellipsoids of the tin atoms in **1** and **2** that are elongated exactly along the $T_d \leftrightarrow S_4$ path of movement (Figure 1, see the Supporting Information).

Concerning the formal oxidation states, C–O bond lengths (i.e., structure analysis), C–O vibrations (i.e., infrared spectra) and DFT-based geometry optimizations, including Mulliken charges, consistently point to iron in $[\{\text{Fe}(\text{CO})_3\}_4\{\text{SnI}_6\text{I}_4\}]^{2-}$ being similar to $\text{Fe}(\text{CO})_5$, and thus with an oxidation state $\text{Fe}^{\pm 0}$. With regard to tin, a formal oxidation state

of $\text{Sn}^{+1.3}$ is expected. This analysis is also consistent with the formal oxidation states $\text{Fe}^{\pm 0}$ and Sn^{+III} that were adopted for a recently discovered barbell-shaped $[\text{FeI}(\text{CO})_3(\text{SnI}_3)_2]^-$ cluster.^[16] In accord with these formal oxidation states, the Fe Mulliken charge^[17] is very similar for $[\{\text{Fe}(\text{CO})_3\}_4\text{SnI}_6]^{2-}$ and $[\text{FeI}(\text{CO})_3(\text{SnI}_3)_2]^-$, whereas the Sn Mulliken charge is much more positive for $[\text{FeI}(\text{CO})_3(\text{SnI}_3)_2]^-$ (Table 3).

Table 3. PBE0/dhf-SVP Mulliken charges^[17] $q(\text{Fe})$ and $q(\text{Sn})$ of $[\{\text{Fe}(\text{CO})_3\}_4\text{SnI}_6]^{2-}$ in comparison with selected reference compounds.

Compound	$q(\text{Fe})$ [e]	$q(\text{Sn})$ [e]
$[\{\text{Fe}(\text{CO})_3\}_4\text{SnI}_6]^{2-}$	−0.87	+0.36
$[\{\text{Fe}(\text{CO})_3\}_4\text{SnI}_6]^{2+}$	−0.92	+0.35
$[\text{FeI}(\text{CO})_3(\text{SnI}_3)_2]^-$	−0.90	+0.52
$\text{Fe}(\text{CO})_5$	−0.89	

To further verify our quantum chemical analysis, we conducted ^{119}Sn Mössbauer spectroscopy studies. Although preparation of 20 mg amounts result in phase-pure $[\text{BIm}][\{\text{Fe}(\text{CO})_3\}_4\text{SnI}_{10}]$ (**1**; FT-IR, TG, EDX), the much larger quantities (> 500 mg) needed for Mössbauer spectroscopy contain the adamantane-like cluster only as a minority phase (Figure 5). This finding can be rationalized based on

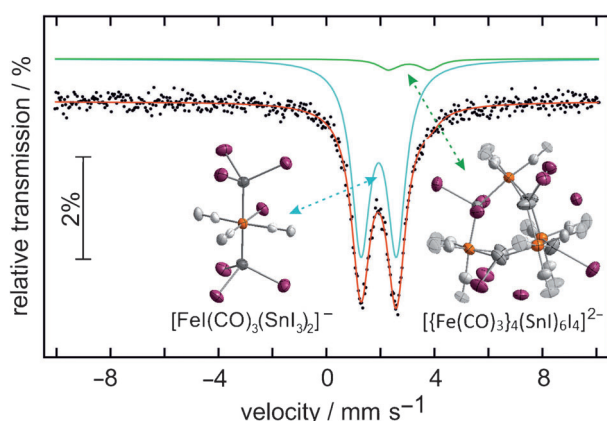


Figure 5. ^{119}Sn Mössbauer spectrum of the adamantane-like $[\{\text{Fe}(\text{CO})_3\}_4\text{SnI}_6]^{2-}$ cluster and the barbell-shaped $[\text{FeI}(\text{CO})_3(\text{SnI}_3)_2]^-$ cluster with transmission integral fit (red) at 78 K (see the Supporting Information).

the reactivity of the starting materials and the resulting carbonyl cluster compounds (see the Supporting Information). The spectra could be well reproduced by a main signal at an isomer shift of $\delta = 1.93(1) \text{ mm s}^{-1}$, exhibiting significant quadrupole splitting of $\Delta E_Q = 1.32(1) \text{ mm s}^{-1}$. This signal stems from the smaller, barbell-shaped $[\text{Fe}^{\pm 0}\text{I}(\text{CO})_3(\text{Sn}^{+III}\text{I}_3)_2]^-$ cluster (see the Supporting Information).^[16] In addition, a weak, quadrupole-split signal at $\delta = 3.0(1) \text{ mm s}^{-1}$ represents the adamantane-like $[\{\text{Fe}(\text{CO})_3\}_4\text{SnI}_6]^{2-}$ cluster (see the Supporting Information). Here, the isomer shift is in good agreement with divalent tin compounds (e.g., SnI_2 :

3.9 mm s^{-1} ; SnO : 2.7 mm s^{-1}) and molecular Fe–Sn clusters (e.g., $[\{(\text{SnCl}_2)\text{Fe}(\text{CO})_4\}_2]$: 2.01 mm s^{-1} ; $[\{(\text{SnBr}_2)\text{Fe}(\text{CO})_4\}_2]$: 2.40 mm s^{-1}).^[18] The quadrupole splitting parameter of $\Delta E_Q = 1.5(1) \text{ mm s}^{-1}$ reflects the non-cubic electron density distribution around the tin nuclei. In sum, the experimental data are again in agreement with approximating a formal oxidation state of $\text{Sn}^{+1.3}$. In addition to ^{119}Sn , we aimed at ^{57}Fe Mössbauer spectroscopy. Owing to the high concentration of iodine, however, the iron atoms are strongly shielded, so that no dedicated signal was obtained. Only a significant enrichment of the sample with ^{57}Fe would solve this problem.

After elucidating the bonding situation and valence state, the question regarding role and benefit of the ionic liquid toward the synthesis of **1** and **2** still remains. In view of their excellent redox stability,^[19] ionic liquids have already been suggested as suitable reaction media for carbonyls. On the other hand, only few studies report on such reactions to date. This includes the synthesis of a tetranuclear $[\{\text{DPIM}\}\text{Co}_2(\text{CO})_6]_2^+$ complex, an imidazolium-based complex $[\text{R}^1\text{ImC}_2\text{HCO}_2(\text{CO})_6]\text{X}$ (X : PF_6^- , BF_4^- , $\text{B}(\text{C}_6\text{H}_5)_4^-$; R^1 : vinyl, allyl) or $[\text{EMIm}]\text{K}[\text{Co}(\text{CO})_4]_2$, in which $[\text{Co}(\text{CO})_4]^-$ units are interlinked by K^+ .^[20] Interestingly, $\text{Co}_2(\text{CO})_8$ was used as a starting material for all the above compounds, whereas $\text{Fe}(\text{CO})_5$ —to our surprise—has not yet been considered as a starting material for the preparation of new carbonyl clusters in ionic liquids. In contrast, its use for the synthesis of Fe^0 nanoparticles has been described recently.^[21] In addition to the redox stability of ionic liquids, their weakly coordinating properties and inertness can also be considered as beneficial aspects.^[20,22] Though, Fe–Sn carbonyl clusters are typically stabilized by alkyl or aryl groups, “purely inorganic” clusters, such as $[\{\text{Fe}(\text{CO})_3\}_4\text{SnI}_6]^{2-}$, have so far been reckoned as less stable.^[2–7]

In summary, the first bimetallic adamantane-like cluster was obtained with $[\{\text{Fe}(\text{CO})_3\}_4\text{SnI}_6]^{2-}$ in the compounds $[\text{BIm}][\{\text{Fe}(\text{CO})_3\}_4\text{SnI}_{10}]$ (**1**) and $[\text{BIm}][\text{S}][\{\text{Fe}(\text{CO})_3\}_4\text{SnI}_{10}]_2$ (**2**). The valence states of iron and tin were verified based on bond-length considerations, FT-IR and ^{119}Sn Mössbauer spectroscopy as well as with DFT calculations. As a result, iron shows an electron density similar to $\text{Fe}(\text{CO})_5$ and can be assumed to exhibit a formal oxidation state of $\text{Fe}^{\pm 0}$. Tin is positively charged and can be estimated to be $\text{Sn}^{+1.3}$. The “purely inorganic” $[\{\text{Fe}(\text{CO})_3\}_4\text{SnI}_6]^{2-}$ cluster in **1** and **2** is not stabilized by alkyl/aryl ligands. Its formation can be ascribed to the synthesis in ionic liquids with their excellent redox stability and their weakly coordinating properties.

Experimental Section

$[\text{BIm}][\{\text{Fe}(\text{CO})_3\}_4\text{SnI}_{10}]$ (1**):** SnI_4 (100 mg, 1 equiv) and $\text{Fe}(\text{CO})_5$ (0.02 mL, 1 equiv) were dissolved in the ionic liquid, $[\text{BIm}][\text{NTf}_2]$. This solution was sealed in a glass ampoule and heated at 130°C for 4 days. After being cooled to room temperature with a rate of 1 K h^{-1} , dark-red crystals of **1** were obtained. The crystals were separated from the ionic liquid by filtration through a glass filter and washed with the pure ionic

liquid to remove the non-reacted starting materials. The crystal size and quality was improved by recrystallization. To this end, **1** (~5 mg) was dissolved in [BMIm][NTf₂] (0.05 mL), [BMIm][OTf] (0.05 mL) and Fe(CO)₅ (0.01 mL), heated to 130 °C for 48 h and cooled to room temperature with a rate of 1 K h⁻¹. By this measure, the phase-pure compound **1** was obtained with about 30 % yield (~2 mg; see the Supporting Information).

[BMIm]₆[S][Fe(CO)₃Sn₄I₁₀]₂ (**2**): SnI₄ (100 mg, 1 equiv), NH₄I (23 mg, 1 equiv) and Fe(CO)₅ (0.02 mL, 1 equiv) were dissolved in the ionic liquid [BMIm][OTf]. This solution was sealed in a glass ampoule and heated at 130 °C for 4 days. Together with colorless crystal needles of [BMIm][SnI₃], dark-red crystals of **2** were obtained after being cooled to room temperature with a rate of 1 K h⁻¹. The addition of NH₄I turned out to be beneficial and improved the crystal size and quality of **2**. Note also that the here-applied ionic liquid [BMIm][OTf] was partially decomposed under the reducing conditions of the carbonyls and led to the formation of yellowish elemental sulfur and sulfide anions. Crystals of **2** were separated from the ionic liquid by filtration through a glass filter. The separation of **2** and [BMIm][SnI₃] was difficult, due to the similar solubility and the high reactivity of **2**. Crystals of **2** needed for further analyses were therefore separated manually.

Interestingly, SnI₄ is required as a reactive starting material for **1** and **2**. This can be ascribed to its Lewis-acid as well as its oxidizing properties. SnI₂ as a starting material, in contrast, did not lead to any reaction with Fe(CO)₅. Further details regarding synthesis and analytical characterization are listed in the Supporting Information.

Acknowledgements

S.W. and C.F. are grateful to Prof. H. Bärnighausen for his very useful suggestions regarding twinning and disorder. S.W., N.M., W.K. and C.F. acknowledge the Center of Functional Nanostructures (CFN) of the Deutsche Forschungsgemeinschaft (DFG) at the Karlsruhe Institute of Technology. F.W. and R.P. are grateful to B. Gerke for help with the ¹¹⁹Sn Mössbauer spectroscopy, and to the DFG.

Keywords: adamantane • carbonyl clusters • cluster compounds • ionic liquids • iron–tin • metal–metal interactions

- [1] Reviews: a) H. Schwertfeger, A. A. Fokin, P. R. Schreiner, *Angew. Chem.* **2008**, *120*, 1038; *Angew. Chem. Int. Ed.* **2008**, *47*, 1022; b) G. Lamoureux, G. Artavia, *Curr. Med. Chem.* **2010**, *17*, 2967.
- [2] J. Fischer, J. Baumgartner, C. Marschner, *Science* **2005**, *310*, 825.
- [3] Review: J. J. Vittal, *Polyhedron* **1996**, *15*, 1585.
- [4] a) R. B. King, F. G. A. Stone, *J. Am. Chem. Soc.* **1960**, *82*, 3833; b) L. Vancea, R. K. Pomeroy, W. A. G. Graham, *J. Am. Chem. Soc.* **1976**, *98*, 1407; c) J. D. Cotton, J. Duckworth, A. R. Knox, P. F. Lindley, I. Paul, F. G. A. Stone, P. Woodward, *J. Chem. Soc. Chem. Commun.* **1966**, *9*, 253; d) P. Braunstein, C. Charles, R. D. Adams, *C. R. Chim.* **2005**, *8*, 1873; e) H. K. Sharma, R. Arias-Ugarte, A. J. Metta-Magana, K. H. Pannell, *Angew. Chem.* **2009**, *121*, 6427; *Angew. Chem. Int. Ed.* **2009**, *48*, 6309; f) L. Zhu, V. Yempally, D. Isrow, P. J. Pellechia, B. Captain, *J. Organomet. Chem.* **2010**, *695*, 1.
- [5] T. J. McNeese, S. S. Wreford, D. L. Tipton, R. Bau, *J. Chem. Soc. Chem. Commun.* **1977**, 390.
- [6] S. G. Anema, B. K. Nicholson, *J. Organomet. Chem.* **1989**, *372*, 25.
- [7] D. Nied, E. Matern, H. Berberich, M. Neumaier, F. Breher, *Organometallics* **2010**, *29*, 6028.
- [8] Fe₃Sn₆I₁₀O₁₂N₄C₂₈H₃₀ (**1**): *M*_r=2819.6, monoclinic, *P*₂₁/*m*, *a*=1156.7(2), *b*=2007.4(4), *c*=1376.5(3) pm, β=107.27(3)°, *V*=3052.1(3)×10⁶ pm³, *Z*=2, ρ(calcd)=3.07 g cm⁻³, μ=8.4 mm⁻¹, *T*=200(1) K; 24593 observed reflections, of which 15079 are independent (*R*_{int}=0.071), 311 parameters, *R*₁=0.046 (*F*_o>4σ(*F*_o)), *wR*₂=0.116 (all data). Fe₈Sn₁₂I₂₀SO₂₄N₁₂C₇₂H₉₀ (**2**): *M*_r=5949.0, rhomboedric, *R*₃, *a*=1997.2(3), *c*=3177.6(6) pm, *V*=10976.7×10⁶ pm³, *Z*=2, ρ(calcd)=1.80 g cm⁻³, μ=4.7 mm⁻¹, *T*=200(1) K; 10150 observed reflections, of which 6961 are independent (*R*_{int}=0.113), 228 parameters, *R*₁=0.033 (*F*_o>4σ(*F*_o)), *wR*₂=0.068 (all data). More information regarding the single crystal structure analysis can be found in the Supporting Information. CCDC-900306 contains the supplementary crystallographic data for this paper. These data can be obtained free of charge from The Cambridge Crystallographic Data Centre via www.ccdc.cam.ac.uk/data_request/cif.
- [9] a) J. M. Cassidy, K. H. Whitmire, *Inorg. Chem.* **1989**, *28*, 2494; b) H. J. Haupt, A. Götze, U. Flörke, *Z. Anorg. Allg. Chem.* **1988**, *557*, 82.
- [10] a) B. Malaman, B. Roques, A. Courtois, J. Protas, *Acta Crystallogr. Sect. B* **1976**, *32*, 1348; b) J. C. Waerenborgh, L. C. J. Pereira, A. P. Gonçalves, H. Noël, *Intermetallics* **2005**, *13*, 490; c) H. J. Wallbaum, *Z. Metallkd.* **1943**, *35*, 218.
- [11] a) R. G. Dickinson, *J. Am. Chem. Soc.* **1923**, *45*, 958; b) R. A. Howie, W. Moser, I. C. Treventa, *Acta Crystallogr. Sect. B* **1972**, *28*, 2965.
- [12] R. D. Shannon, *Acta Crystallogr. Sect. A* **1976**, *32*, 751.
- [13] a) J. Donohue, A. Caron, *J. Phys. Chem.* **1967**, *71*, 777; b) B. Beagley, D. W. J. Cruickshank, P. M. Pinder, A. G. Robiette, G. M. Sheldrick, *Acta Crystallogr. Sect. B* **1969**, *25*, 737.
- [14] J. Pipeke, P. G. Mezey, *J. Chem. Phys.* **1989**, *90*, 4916.
- [15] S. F. Boys, in *Quantum Theory of Atoms, Molecules and the Solid State* (Ed.: P.-O. Löwdin), Academic Press, New York, **1966**, p. 253.
- [16] S. Wolf, F. Winter, R. Pöttgen, N. Middendorf, W. Klopfer, C. Feldmann, *Dalton Trans.* **2012**, *41*, 10605.
- [17] R. S. Mulliken, *J. Chem. Phys.* **1955**, *23*, 1833.
- [18] a) P. E. Lippens, *Phys. Rev. B* **1999**, *60*, 4576; b) A. B. Cornwell, P. G. Harrison, *J. Chem. Soc. Dalton Trans.* **1975**, 2017.
- [19] a) P. Wasserscheid, T. Welton, *Ionic Liquids in Synthesis*, Wiley-VCH, Weinheim, **2008**; Review: b) D. Freudenmann, S. Wolf, M. Wolff, C. Feldmann, *Angew. Chem.* **2011**, *123*, 11244; *Angew. Chem. Int. Ed.* **2011**, *50*, 11050; Review: c) E. Ahmed, M. Ruck, *Dalton Trans.* **2011**, *40*, 9347.
- [20] a) H. Schottenberger, K. Wurst, U. E. I. Horvath, S. Cronje, J. Lukasser, J. Polin, J. M. McKenzie, H. G. Raubenheimer, *Dalton Trans.* **2003**, 4275; b) F. G. Deng, B. Hu, W. Sun, C. G. Xia, *Dalton Trans.* **2008**, 5957.
- [21] a) C. Vollmer, E. Redel, K. Abu-Shandi, R. Thomann, H. Manyar, C. Hardacre, C. Janiak, *Chem. Eur. J.* **2010**, *16*, 3849; b) J. Krämer, E. Redel, R. Thomann, C. Janiak, *Organometallics* **2008**, *27*, 1976.
- [22] Reviews: a) I. Krossing, I. Raabe, *Angew. Chem.* **2004**, *116*, 2116; *Angew. Chem. Int. Ed.* **2004**, *43*, 2066; b) S. Bulut, P. Klose, M. M. Huang, H. Weingärtner, P. J. Dyson, G. Laurenczy, C. Friedrich, J. Menz, K. Kümmerer, I. Krossing, *Chem. Eur. J.* **2010**, *16*, 13139.

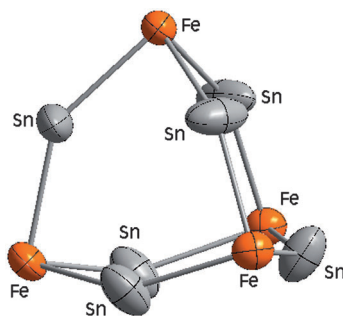
Received: July 26, 2012
Published online: ■ ■ ■, 0000

Cluster Compounds

S. Wolf, F. Winter, R. Pöttgen,
N. Middendorf, W. Kloppe,
C. Feldmann* ■■■■–■■■■



$[\{\text{Fe}(\text{CO})_3\}_4\{\text{SnI}\}_6\text{I}_4]^{2-}$: The First Bimetallic Adamantane-Like Cluster



Show some metal: The first bimetallic adamantane-like cluster, $[\{\text{Fe}(\text{CO})_3\}_4\{\text{SnI}\}_6\text{I}_4]^{2-}$ (see structure), was prepared by ionic-liquid-based synthesis. The valence states of iron and tin were verified based on bond-length considerations, FT-IR and ^{119}Sn Mössbauer spectroscopy as well as with DFT calculations.